Diffusive shock acceleration at laser-driven shocks: studying cosmic-ray accelerators in the laboratory

Published in:
New Journal of Physics

Document Version:
Publisher's PDF, also known as Version of record

Queen's University Belfast - Research Portal:
Link to publication record in Queen's University Belfast Research Portal

Diffusive shock acceleration at laser-driven shocks: studying cosmic-ray accelerators in the laboratory

You may also be interested in:

New Journal of Physics

Diffusive shock acceleration at laser-driven shocks: studying cosmic-ray accelerators in the laboratory

B Reville[1], A R Bell and G Gregori

Clarendon Laboratory, Parks Road, Oxford OX1 3PU, UK
E-mail: b.reville1@physics.ox.ac.uk

Abstract. The non-thermal particle spectra responsible for the emission from many astrophysical systems are thought to originate from shocks via a first order Fermi process otherwise known as diffusive shock acceleration. The same mechanism is also widely believed to be responsible for the production of high energy cosmic rays. With the growing interest in collisionless shock physics in laser produced plasmas, the possibility of reproducing and detecting shock acceleration in controlled laboratory experiments should be considered. The various experimental constraints that must be satisfied are reviewed. It is demonstrated that several currently operating laser facilities may fulfil the necessary criteria to confirm the occurrence of diffusive shock acceleration of electrons at laser produced shocks. Successful reproduction of Fermi acceleration in the laboratory could open a range of possibilities, providing insight into the complex plasma processes that occur near astrophysical sources of cosmic rays.

[1] Author to whom any correspondence should be addressed.

IOP Institute of Physics ⏀ DEUTSCHE PHYSIKALISCHE GESELLSCHAFT

Contents

1. Introduction

The theory of diffusive shock acceleration was independently put forward in four publications in the late seventies [2, 4, 10, 27] as a mechanism to account for the non-thermal emission from astrophysical shocks and also as a possible explanation for the origin of cosmic rays. A particularly attractive feature of this process is that, in the simplest test-particle theory, the accelerated particles naturally form power-law spectra consistent with those inferred from multi-wavelength measurements. Despite the success of this theory in explaining observations covering a broad range of astrophysical phenomena, from interplanetary and supernova remnant shocks to radio galaxy hotspots and γ-ray bursts, a complete understanding of the mechanism is still lacking. Theoretical models and numerical simulations have developed rapidly over the last 30 years, however, the limited data provided by *in situ* satellite measurements at shocks in our solar system make verification of these models difficult. The ability to successfully perform experiments to study diffusive shock acceleration in controlled laboratory environments would represent a major advance in the field.

Modern high-power laser facilities provide the means to generate strong shocks in the laboratory. These facilities are already being used to perform experiments in a parameter range where scaling relations may be used to apply results to plasma physics studies of astrophysical relevance [19, 33, 44]. The conditions required to make comparisons with astrophysical shocks has been the focus of several papers, e.g. [13, 36, 44]. While several laser–plasma experiments have focused on the generation and analysis of collisionless shocks [12, 28, 29, 35], to date there has been no report of a successful detection of shock acceleration. We review the relevant results of the theory primarily in the context of laboratory laser-driven shocks. The extension to other plasma experiments, such as on the plasma railgun device at the Los Alamos National Laboratory [21] is straightforward. The constraints on plasma parameters necessary to accelerate and more importantly, detect energetic particles are discussed in detail. It is demonstrated that the required conditions can in principle be satisfied for several current laser

facilities, and that experiments designed to detect accelerated particles could be carried out in the very near future.

2. Shock acceleration

The acceleration of particles in a conducting fluid requires an electric field. For laboratory plasmas, neglecting resistivity, a typical form for Ohm's law is $\boldsymbol{E} = -\boldsymbol{u}_e \times \boldsymbol{B} - \nabla p_e / n_e e$, with u_e, p_e and n_e the electron fluid velocity, pressure and number density respectively. On length scales $L \gg v_{\mathrm{th,e}}^2 / u_0 \omega_{\mathrm{ce}}$, where $v_{\mathrm{th,e}}$ and ω_{ce} are the electron thermal velocity and cyclotron frequency respectively, and u_0 a characteristic velocity of the background fluid, the pressure gradient can be neglected, and the large-scale electric field vanishes in the local plasma fluid frame. This is the situation usually considered in astrophysical plasmas. Since the fluid velocity is seldom uniform on large scales, the electric field does not vanish globally, and, as a consequence, a charged particle with sufficient momentum to decouple from the thermal plasma associated with the local fluid motion, can sample the global electric field and accelerate to higher energy. This is the underlying principle of Fermi acceleration [15]. While this process is typically quite slow in the presence of small velocity fluctuations, at shock fronts, where the incoming fluid is abruptly decelerated and compressed, the acceleration can be very rapid. The process by which a distribution of particles repeatedly samples this velocity jump is known as diffusive shock acceleration (for detailed reviews, see e.g. [9, 14]).

The efficacy of the acceleration hinges on a particle's ability to cross the shock surface many times, since the increase in energy on each crossing is relatively small. For a shock velocity u_{sh} and particle velocity v ($\gg u_{\mathrm{sh}}$), the fractional increase in energy on each crossing is of order u_{sh}/v. Acceleration to high energies relies on a number of conditions. Firstly, as mentioned above, the particle must have a sufficiently large initial momentum to *escape* from the thermal pool and overtake the shock. This is the so-called injection problem, and remains a topic of ongoing investigation (see [1, 26, 34] and references therein). Secondly, the scattering must be sufficiently frequent to maintain near isotropic particle distributions. For acceleration to proceed these scatterings must be mediated by quasi-elastic interactions with magnetic fluctuations, as opposed to inelastic Coulomb collisions with other particles. The scattering fluctuations in a laboratory setting can be produced for example via Weibel instability in the shock layer [25, 37], or hydromagnetic waves excited by shock reflected or accelerated particles [5, 6]. If a small fraction of the particles crossing the shock are heated to super-thermal velocities, provided these particles are maintained approximately isotropic, the probability of a particle interacting with the shock multiple times is high.

2.1. Acceleration time

Assuming the above mentioned conditions can be satisfied, at an idealized shock, the resulting acceleration timescale is [14]

$$t_{\mathrm{acc}} = \frac{3}{u_{\mathrm{u}} - u_{\mathrm{d}}} \left(\frac{D_{\mathrm{u}}}{u_{\mathrm{u}}} + \frac{D_{\mathrm{d}}}{u_{\mathrm{d}}} \right), \tag{1}$$

where $u_{\mathrm{u,d}}$ are the upstream and downstream flow velocities as measured in the shock rest frame, and $D_{\mathrm{u,d}}$ the corresponding energy dependent diffusion coefficient in the direction normal

to the shock surface. The diffusion coefficient can vary quite significantly depending on the inclination of the shock normal with respect to the local magnetic field. From scaling arguments, it is clear that fast shocks with small diffusion coefficients are more rapid accelerators. Since cross–field diffusion is much less effective than diffusion along magnetic field lines ($D_\perp \ll D_\parallel$), perpendicular shocks, i.e. shocks for which the incoming magnetic field is in a direction perpendicular to the direction of the shock's motion, can have considerably shorter acceleration times [24]. From an experimental perspective, minimizing the acceleration time is crucial, since as we will show in section 3.1, the time window for making detections is narrow even in the most optimistic scenario. In addition, the acceleration rate is always competing with Coulomb collisions at low energies. We therefore focus on the acceleration of particles at perpendicular shocks.

In the quasi-linear approximation [23], the diffusion can be separated into two orthogonal components, parallel and perpendicular to the mean field:

$$D_\parallel = \frac{D_B}{\xi} \quad \text{and} \quad D_\perp = \frac{\xi D_B}{1 + \xi^2},$$

where $\xi = (\omega_g \tau_B)^{-1} < 1$ is the ratio of the effective collision rate, τ_B^{-1}, to the gyrofrequency, and

$$D_B = \frac{mcv^2}{3eB} \tag{2}$$

is the (non-relativistic) Bohm diffusion limit, corresponding to roughly one scattering per gyroperiod. Here τ_B is the mean time between collisions on magnetic fluctuations, not to be confused with Coulomb interactions. The value of ξ will depend on the value of the background field and also the level and scale of magnetic fluctuations. A typical scale for fluctuations in the plasma is the electron collisionless skindepth, although magnetized shock experiments have shown evidence for structures on the scale of the hot electrons' gyroradius [12]. For typical laboratory conditions, e.g. $B = 1\,\text{T}$, $n = 10^{16}\,\text{cm}^{-3}$, these scales are comparable at electron temperatures of $400\,\text{eV}$ (see section 3.4).

For perpendicular shocks, it is the details of the magnetic fluctuations in the immediate vicinity of the shock that determines the acceleration. If scattering is too weak ($\omega_g \tau_B \gg 1$), particles are tied to the field lines and are advected downstream preventing further interaction with the shock, and thus are not accelerated efficiently [7]. If the scattering is too strong, ($\omega_g \tau_B \to 1$), the diffusion is approximately isotropic. In this case the direction of the magnetic field becomes insignificant, particles can make long excursions both upstream and downstream before returning to the shock, and the acceleration time correspondingly increases. The optimal value for acceleration at a perpendicular shock is $\omega_g \tau_B = v/u_{sh}$ [24] although in practice it may be less than this. We will adopt the optimal value for most of the calculations that follow, since at high energies, provided $\omega_g \tau_B \gg 1$, geometry plays the limiting role, while at low energies v/u_{sh} is not very large and any correction is likely to be of order unity.

2.2. Maximum energy

In the absence of radiative (synchrotron, bremsstrahlung etc) or adiabatic cooling, the maximum energy to which a particle can be accelerated is limited either by time or geometry. For acceleration at perpendicular shocks, we can demonstrate that the acceleration time is shorter

than the hydrodynamic time, and thus the geometry plays the key role. In astrophysics, this limit is commonly referred to as the Hillas criterion [20], and corresponds to the maximum potential difference a particle can experience in a system of fixed size

$$T_{\max} \approx eER_{\mathrm{sh}} \approx e|\boldsymbol{B}|(u_{\mathrm{sh}}/c)R_{\mathrm{sh}} \approx B_4\, u_{\mathrm{sh},7}\, R_{\mathrm{sh}}\, \mathrm{keV}, \tag{3}$$

where $B = B_4 \times 10^4\,\mathrm{G}$ is the strength of the magnetic field, $u_{\mathrm{sh}} = u_{\mathrm{sh},7} \times 10^7\,\mathrm{cm\,s^{-1}}$ is the shock velocity and R_{sh} is the shock radius in cm. The same subscript notation is used throughout the paper. For perpendicular shocks, inserting (3) into (1) gives $u_{\mathrm{sh},7}t_{\mathrm{acc}}(T_{\max}) \approx \xi R_{\mathrm{sh}}$, such that our assumption on geometry limited acceleration is consistent (since $\xi < 1$). To make an unambiguous detection of shock accelerated particles, we require as large a separation as possible between $T_{\max}$ and the injection energy. This is discussed further in the next section.

3. Practical considerations

Most astrophysical shocks of interest are highly collisionless systems. Such shocks are generally believed to be excellent particle accelerators. Achieving similar collisionless conditions in the laboratory however is not straightforward, and places stringent limitations on experiments designed to reproduce shock acceleration. While the total energy will depend on the maximum laser energy that a given system can provide, the external conditions must also satisfy a number of criteria. As outlined in the previous section, a mean field is necessary to prevent particles escaping far upstream. There have been a number of experiments designed to study collisionless magnetized shocks [12, 44], using conditions relevant for scaling to supernova shocks. An interesting outcome of these experiments of vital importance here was the observation that very little penetration of the magnetic field into the shocked plasma occurred. Compression of the magnetic field is almost certainly required to accelerate rapidly to high energies (see figure 1).

Since the focus here is not to produce scaled versions of supernovae, but rather to study acceleration from first principles, and to help the magnetic field lines penetrate the plasma, we consider an alternative experimental set-up to that of [12, 44] based on the previous experimental design of [19]. In this design, the laser or lasers are focused onto a central target in a neutral-gas filled chamber, driving a quasi-spherical shock into the ambient gas. Since the magnetic field already penetrates the ambient gas before the shock arrives, provided the gas is ionized sufficiently far upstream of the shock, there should be no issue with the magnetic field penetrating the plasma or preventing it from being advected downstream.

We now discuss in detail the constraints on density and magnetic field strength for a given laser energy in the context of shock acceleration.

3.1. Energy budget

The total energy available to the expanding shock is the principal limiting factor for any shock acceleration experiment, as already evident from equation (3). For a spherical explosion, the shock undergoes a short-lived ballistic expansion before evolving to a Sedov–Taylor expansion $R_{\mathrm{sh}} \propto t^{2/5}$. In this phase, the shock is already decelerating $u_{\mathrm{sh}} \propto t^{-3/5} \propto R_{\mathrm{sh}}^{-3/2}$. Inserting this scaling into equation (3), for a constant magnetic field, the maximum energy decreases with time $\propto t^{-1/5}$. Thus, once the expansion velocity is determined, the maximum energy at a given distance can be inferred from equation (3).
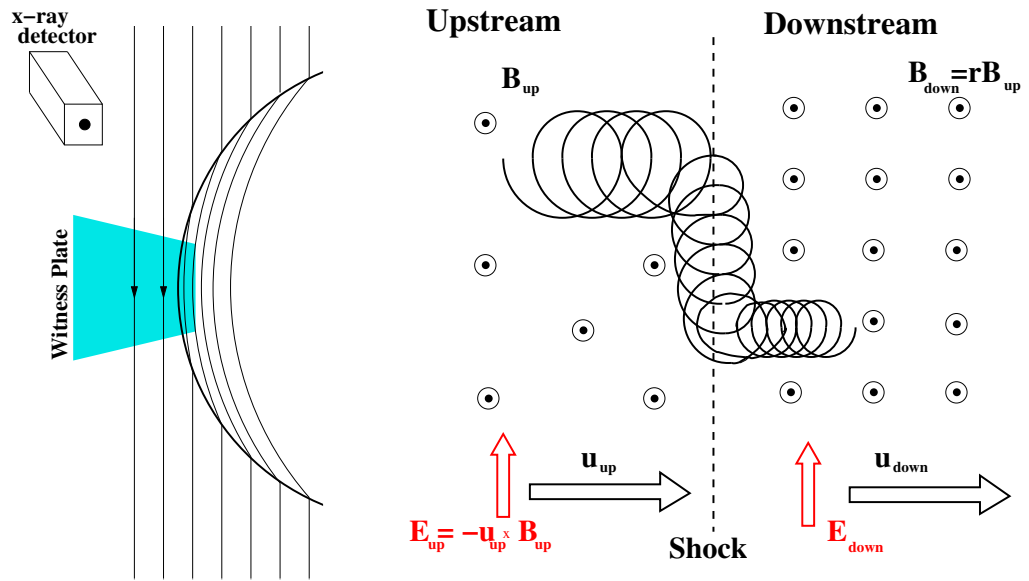
Figure 1. Left: edge on view, showing spherical shock wave in uniform magnetic field. In the absence of magnetic diffusion, the tangential component of the magnetic field is compressed at a strong shock by a factor $r = (\gamma + 1)/(\gamma - 1)$. Right: side view of a small section of the shock where field is purely perpendicular. Electrons experience a grad B drift along the surface of the shock as a result of the magnetic field compression. In this example, we have assumed no scattering, and the particles are accelerated by the shock drift mechanism [43]. Small angle scattering on magnetic fluctuations allow some particles to 'hug' the shock surface for a hydrodynamic timescale (see section 2.1). The preferred direction of the accelerating electrons can be used to detect the presence of shock acceleration.

For a given experiment, the total deposited laser energy is divided up into the production of radiation, ionization of the external medium, magnetic energy, thermal energy and shock accelerated particles, if present. For low Z gases such as helium at densities $n \ll 10^{18} \, \text{cm}^{-3}$, the radiative cooling is dominated by bremsstrahlung, however, for the experimental set-up we consider here, the cooling time is much longer than the dynamical time [36]. At low densities, the ionization potential is typically smaller than the thermal energy density, and so can be neglected. Hence, to a good approximation we can assume a typical Sedov–Taylor solution

$$R_{\text{sh}} = C_0 \left(\frac{E_0 t^2}{\rho_{\text{ext}}} \right)^{1/5}, \tag{4}$$

where E_0 is the total energy in the blast-wave, ρ_{ext} the gas density in the target chamber and for helium gas, the numerical constant is $C_0 \approx 1.15$. For laser plasma interactions, while a large fraction of the laser energy is absorbed by the target, the fraction of this energy that goes into the blast-wave is uncertain. Comparing with similar spherical blast-wave experiments such as those carried out in [19], $E_0 = 0.01 E_{\text{laser}}$ provides an excellent fit to the data, however, careful target design may increase this number. We parameterize the fraction of the laser energy transferred to the blast-wave as $E_0 = 10^{-2} \eta_{-2} E_{\text{laser}}$ and leave η_{-2} as a free parameter. The shock velocity at

distance R_{sh} is therefore

$$u_{sh,7} \approx 6 \frac{\eta_{-2}^{1/2} E_{kJ}^{1/2}}{n_{16}^{1/2} R_{sh}^{3/2}}, \tag{5}$$

where E_{kJ} is the total laser energy in kilo Joules and n_{16} the external gas number density in units 10^{16} cm^{-3}. Combining with equation (3), and assuming a helium filled target chamber, the maximum energy as a function of distance is

$$T_{max} \approx 6 \, \eta_{-2}^{1/2} \, B_4 \, E_{kJ}^{1/2} \, n_{16}^{-1/2} \, R_{sh}^{-1/2} \, \text{keV}. \tag{6}$$

As pointed out by Drake [13], a slowly diverging plasma expansion such as the 'laser-driven rocket', can drive a shock at high velocity over a longer distance. However, we note that the gain in time is nearly balanced by the reduction in T_{max}, since the maximum energy is determined by the lateral extent of the shock. Alternatively a hemispherical blast-wave could be generated, although the maximum energy would only change by a factor of $\sim \sqrt{2}$.

3.2. Magnetic field

Following the discussion in section 2.1, it is clear that having a strong magnetic field is advantageous. It increases both the acceleration rate and the maximum energy. However, even in the presence of efficient scattering, there is a limit on the maximum magnetic field that permits acceleration. This additional constraint on the external medium, is that the magnetic pressure $B^2/4\pi$, should not exceed the shock ram pressure $\rho_{ext} u_{sh}^2$. This is equivalent to saying that the shock is super-Alfvénic, $M_A > 1$. Inserting numerical quantities, the necessary condition is

$$n_{16}^{1/2} \, u_{sh,7} \, B_4^{-1} > 1. \tag{7}$$

Since the expected density and magnetic field are approximately constant in the experiment, this condition will ultimately be violated when the shock has decelerated appreciably.

3.3. Collisions and magnetic diffusivity

A prerequisite for shock acceleration is that the particles approximately conserve energy between shock crossings. For this to occur, Coulomb collisions must be negligible for the accelerating particles. For rapid acceleration at perpendicular shocks the pathlength on either side of the shock is on the order of its gyroradius. The ratio of the Coulomb mean free path, λ_{mfp}, of an electron to its gyroradius is, assuming a Coulomb logarithm $\ln\Lambda \sim 10$ [22],

$$\frac{\lambda_{mfp}}{r_g} \approx 0.6 \, B_4 \, n_{16}^{-1} \, T_e^{3/2}, \tag{8}$$

where T_e is the electron temperature in eV. Since this ratio grows rapidly with electron energy, it is sufficient to demonstrate that collisions are negligible at the injection energy. The equivalent ratio for protons is approximately $\sqrt{m_e/m_p}$ times smaller, making the acceleration of protons far more difficult. To achieve acceleration, we require the associated acceleration time at the injection energy be shorter than the inverse of the Coulomb scattering frequency. Adopting the previously discussed optimal scattering rate $\xi = u_{sh}/v$, the necessary condition

for Coulomb scattering to be unimportant can be expressed as $\lambda_{\mathrm{mfp}}/r_{\mathrm{g}} \gg v/u_{\mathrm{sh}}$, which together with equation (8) gives[2]

$$B_4 \, n_{16}^{-1} \, T_{\mathrm{e}} \, u_{\mathrm{sh},7} \gg 0.1. \tag{9}$$

If the scattering rate is closer to unity, the acceleration rate decreases, and the minimum injection energy must increase accordingly. In the other extreme, where cross field diffusion becomes negligible ($\xi \ll u_{\mathrm{sh}}/v$), acceleration can not occur. In this scenario, seeding of electric and magnetic fluctuations may be achieved using fast electrons (see the next section).

For a strong shock, the downstream temperature of the shocked ions, in this case helium, is, according to the Rankine–Hugoniot relations, $T_{\mathrm{i}} \approx 75 u_{\mathrm{sh},7}^2$ eV. The downstream electron temperature may be as much as $m_{\mathrm{e}}/m_{\mathrm{p}}$ times smaller than this, although there is considerable observational evidence that in collisionless shocks, this ratio ($T_{\mathrm{e}}/T_{\mathrm{i}}$) is closer to 0.1 [39, 41]. In addition, it seems likely that even for mildly collisional shocks, a small fraction of the electrons can still be heated to considerably higher energies due to the collective processes in the shock layer, and satisfying (9).

The role of collisions and the resulting magnetic diffusivity may also be important. If the magnetic Reynolds number is not appreciably greater than unity, the ability of the flow to distort and compress the magnetic field is severely limited. This can dramatically reduce the efficiency of shock acceleration. Examination of (8) reveals however, that even modest temperatures of a few eV are sufficient to magnetize the electrons. Electron temperatures similar and considerably larger than this have already been produced in previous experiments [19, 32], and this is unlikely to present a serious limitation.

3.4. Particle injection

In both astrophysical and laboratory shocks, perhaps the biggest uncertainty in the theory of shock acceleration is how and in what quantity particles are lifted from the thermal background and injected into the acceleration process [26]. If the shock is indeed collisionless, we can put some estimates on critical length and energy scales of the problem. For collisionless shock experiments, a crucial parameter is the collisionless skin-depth

$$\lambda_{\mathrm{SD}} = \frac{c}{\omega_{\mathrm{pe}}} \approx 50 \, n_{16}^{-1/2} \, \mu\mathrm{m}. \tag{10}$$

With the gyroradius of an electron in such an experiment $r_{\mathrm{g}} \approx 75 T_{\mathrm{keV}}^{1/2}/B_4 \, \mu\mathrm{m}$, it follows that electrons with energy $T_{\mathrm{e}} \sim 400 B_4/n_{16}$ eV will interact resonantly with structures on this scale, and it might be expected for a collisionless shock, a fraction of particles will be naturally heated to such temperatures. For perpendicular shocks, there are a number of collective mechanisms believed to preheat the electrons, e.g. lower hybrid waves [8, 31], whistler waves [1, 34] or indeed the collective processes mediating the shock itself [37]. Recent kinetic simulations are advancing our knowledge of different electron injection mechanisms at collisionless shocks [1, 17, 34], however, a complete theory is still lacking. Nevertheless, there is a great deal of observational evidence supporting the fact that the bulk electron temperature downstream can be on the order of 10% that of the ions, which may be sufficient for electrons to escape upstream.

---

[2] Repeating the same calculation for protons, we require $B_4 n_{16}^{-1} T_{\mathrm{p}} u_{\mathrm{sh},7} \gg 100$. While this condition can be satisfied at a fast shock, any accelerated protons will be indistinguishable from simply shock heated protons.

In practice, we only require a small fraction of the incoming electrons to achieve such high energies.

The uncertainty associated with injection is evident, and cannot be relied upon. This clearly emphasizes the need to have an alternative mechanism in place should it be needed. One such possibility is to inject a population of energetic electrons at early times. While this may be experimentally challenging and entails a certain amount of fine tuning, it should be possible. The generation of fast electrons using an external source is easily achieved by irradiating an additional target. The mean kinetic energy and total flux of fast electrons are also straightforward to calibrate [3, 18]. However, fast electrons are known to produce their own electric and magnetic fields as they propagate, potentially influencing the acceleration of particles. Provided the fields produced saturate with total energy density less than that of the ambient magnetic field, the acceleration will still be dominated by the zeroth order field. This effect can be calibrated with control shots in the absence of a shock. However, the enhanced turbulence level may also increase the cross-field diffusion, thus reducing the acceleration rate. The magnitude of this effect is entirely model specific, but is not entirely unjustified in an astrophysical context. Most astrophysical shocks are known to excite instabilities upstream of the shock due to cosmic-ray or shock reflected ion currents. While this is an interesting and topical area in cosmic-ray acceleration research, if the aim is to study the acceleration mechanism in its simplest test-particle form, the fast electron flux should be calibrated, so as to minimize this effect. The fast electrons should also be timed to intersect with the shock as early as possible, subject to the condition $r_g < R_{sh}$.

4. Necessary conditions for detection

The necessary requirements to achieve shock acceleration have been detailed in the previous section. However, as has been regularly emphasized, the key objective is to produce an unambiguous detection. The main requirements are contained in equations (6), (7) and (9). Supplementing these conditions with the assumption that some fraction of the electrons are heated to an energy T_{inj} approximately 10% that of the shocked ions, $T_{inj} = 0.1\alpha T_i = 7.5\alpha u_{sh,7}^2$ eV and shock velocity

$$u_{sh,7} = 6\frac{\eta_{-2}^{1/2} E_{kJ}^{1/2}}{n_{16}^{1/2} R_{sh}^{3/2}},$$

the velocity can be eliminated from the above conditions, and the most relevant dimensionless quantities are

$$M_A = 6\frac{\eta_{-2}^{1/2} E_{kJ}^{1/2}}{B_4 R_{sh}^{3/2}}; \quad \left.\frac{t_{coll}}{t_{acc}}\right|_{T_{inj}} = 245\alpha\frac{B_4 \eta_{-2}^{3/2} E_{kJ}^{3/2}}{n_{16}^{5/2} R_{sh}^{9/2}}; \quad \frac{T_{max}}{T_{inj}} = 20\frac{B_4 n_{16}^{1/2} R_{sh}^{5/2}}{\alpha\eta_{-2}^{1/2} E_{kJ}^{1/2}}.$$

Taking reasonably conservative minimal requirements, the experimental parameters must satisfy the following inequalities.

(i) Super-Alfvénic ($M_A > 4$)

$$R_{sh} < 1.3\frac{\eta_{-2}^{1/3} E_{kJ}^{1/3}}{B_4^{2/3}} \text{ cm.}$$

(ii) Injected electrons are collisionless ($t_{coll} > 10 t_{acc}$)

$$R_{sh} < 2 \, \frac{\alpha^{2/9} \eta_{-2}^{1/3} E_{kJ}^{1/3} B_4^{2/9}}{n_{16}^{5/9}} \, \text{cm}.$$

(iii) Significant gain ($T_{max} > 10 T_{inj}$)

$$R_{sh} > 0.75 \, \frac{\alpha^{2/5} \eta_{-2}^{1/5} E_{kJ}^{1/5}}{B_4^{2/5} n_{16}^{1/5}} \, \text{cm}.$$

As can clearly be seen, detecting electron acceleration using a kilo-Joule facility has a small window for success, since a clear distinction between background and thermal particles sets a lower bound on the shock position, while the remaining conditions set upper bounds. As an example, consider an experiment where we achieve the conditions such that all normalized quantities (E_{kJ}, B_4 etc) are unity. The above inequalities are satisfied for $0.75 \, \text{cm} < R_{sh} < 1.3 \, \text{cm}$. Increasing the laser energy to values relevant for facilities such as Omega, and in particular the National Ignition Facility (NIF), increases the available time window, although the weak dependence of the upper and lower bounds on laser energy (to the 1/3 and 1/5 power respectively) imply only a marginal increase.

5. Diagnostics

While the necessary conditions for detection have been outlined, a method for measuring the presence of accelerated particles has so far not been discussed. To this end, accurate diagnostics of the plasma parameters are essential. The plasma density, temperature and magnetic field strength can be probed using standard techniques such as interferometry, Thomson scattering and Faraday rotation. In addition, Schlieren imaging can be used to determine the shock velocities.

Determining the presence of the non-thermal particles is more challenging. The electrons should be detected in the range of R_{sh} determined in the previous section, since at large radii the adiabatic losses of the particles in the expanding plasma is important. Taking conditions (ii) and (iii) in the previous section, the maximum energy electrons are expected in the range

$$3.8 \frac{\eta_{-2}^{1/3} E_{kJ}^{1/3} B_4^{8/9}}{n_{16}^{2/9}} < T_{max}(\text{keV}) < 7 \, \frac{\eta_{-2}^{2/5} E_{kJ}^{2/5} B_4^{6/5}}{\alpha^{1/5} n_{16}^{2/5}}$$

with the shock heated electrons T_{inj}, also by condition (iii), an order of magnitude smaller. The maximum energy electrons are expected to fall in the range where it is possible to make use of the radiative Auger effect [11]. A high Z metal witness plate placed at the appropriate location can thus be used as a probe of the accelerated electrons, as shown in left image of figure 1. Alternatively, the target chamber plasma could be doped with high Z gas such as argon (with $n_{Ar}/n_{16} = f \sim 0.01$) that could show enhancement of inner shell emission near the shock. Both these approaches may be quite sensitive to injection efficiency. Assuming an injection efficiency of $\chi \sim 10^{-4}$, i.e. 10^{-4} of the upstream electrons crossing the shock per unit time are injected into the acceleration process, and assuming the test-particle solution for diffusive shock accelerated particles: $dN(T) \propto T^{-2} \, dT$, the number of electrons at T_{max} is

$$N(T_{max}) \approx 10^{12} \chi_{-4} n_{16} \left(\frac{T_{max}}{T_{inj}} \right)^{-2} \sim 10^{10} \chi_{-4} n_{16},$$

where we have again taken $T_{max} = 10 T_{inj}$. The Ar inner shell ionization cross section peaks at $\sim 5\,keV$ ($\sigma_{iz} = 3 \times 10^{-21}\,cm^2$ [38]), and assuming a fluorescence yield $Y_K \sim 0.14$ [42], the estimated number of photons collected within the detector solid angle $\Omega \sim 0.1\,sr$ is

$$N_{ph} \approx 3 \times 10^{25} f \, Y_K \, \chi_{-4} \, \Omega \, \sigma_{iz} \, R_{sh}^4 \, n_{16}^2,$$

which gives $N_{ph} \sim 4$–35 for shock radii considered here. While small, this number is sufficient for single shot detection, especially if a high throughput crystal monochromator is used to enhance the signal to noise ratio.

Another possible technique that may be used to make a detection, involves taking advantage of the perpendicular geometry. At a perpendicular shock, the acceleration has a directional bias, determined by the grad B drift, as shown in figure 1. The resulting asymmetry in the x-ray luminosity on opposite sides of the witness plate could be detected using two pinhole x-ray cameras.

In all cases, care should be taken not to confuse any signal from fast electrons produced either from the laser–target interaction, or stray electrons from the external injection source. Again, control experiments can be used to confirm or invalidate any successful detections.

6. Discussion

The theory of diffusive shock acceleration has been incredibly successful in accurately modelling non-thermal radiation from astrophysical sources for several decades. While the evidence for its occurrence at numerous shocks in both astrophysical and space environments is convincing, there are many aspects that can not be fully understood from distant observations and satellite measurements. In particular questions about injection, self-regulation, maximum energy, nonlinear feedback and magnetic field amplification are active areas of research in the theoretical community. The study of collisionless shocks using high-power lasers is a growing field [12, 28, 29, 35, 44], and the question of whether shock acceleration, or the formation of non-thermal particle populations occurs, is of fundamental importance.

We have reviewed the necessary conditions that must be satisfied in order to achieve a clear detection of accelerated particles. Our analysis confirms that several laser facilities currently operating may be capable of producing a shock which accelerates electrons to maximum energies where they can be clearly distinguished as shock accelerated particles. It is however quite unlikely that the same can be done for protons for any currently existing facilities. We also note that the requirement that the shock be completely collisionless can be relaxed slightly, although it remains crucial that the magnetic Reynolds number is sufficiently large that the magnetic dissipation can be neglected on the gyro-scale of the accelerating electrons.

There are a number of uncertainties in the analysis presented in this paper, about which we have tried to be transparent. However, we can summarize them here again. Firstly the question of injection, which is also of great importance in astrophysics. We have made the, not unreasonable, approximation that a small fraction of the shocked electrons are heated to a temperature on the order of 10% that of the shocked ions. While this assumption is of course arbitrary, if no acceleration is observed, it is still possible to inject fast electrons that satisfy the necessary conditions. On the other hand, should acceleration be detected without external injection, these experiments provide a novel platform to study the injection itself.

The other major uncertainty is the nature of the scattering $\omega_g \tau_B$. This is an important topic in its own right in the study of collisionless shocks, and recent experiments are advancing our

IOP Institute of Physics ⬡ DEUTSCHE PHYSIKALISCHE GESELLSCHAFT

understanding [28, 35]. However, as noted earlier, the ratio of the gyroradius of a keV electron to the collisionless skin-depth is $r_g(\text{keV})/(c/\omega_{pe}) = 1.4 B_4^{-1} n_{16}^{1/2}$, i.e. on the correct scale to scatter resonantly the electrons. Future magnetized experiments will provide valuable information.

While the discussion in this paper has involved, in all cases, the presence of a strong large-scale field, there are ongoing efforts to realize collisionless unmagnetized shocks in the laboratory [28, 32]. Numerical simulations of unmagnetized shocks, in an astrophysical context, have developed rapidly in recent years [25, 30, 40], and are of vital importance to understanding the underlying kinetic processes. However, for the non-relativistic flow speeds we expect in the laboratory, our analysis suggests that a large-scale magnetic field is required to accelerate particles to energies where a detection can be made on the relevant timescale. The production of mildly relativistic unmagnetized shocks in the laboratory has recently been demonstrated numerically [16], using particle-in-cell simulations of intense (10^{20}–$10^{22}\,\text{W}\,\text{cm}^{-2}$) laser pulses in an over-dense plasma. This is an exciting line of research with many applications, however, regarding shock acceleration, the finite lifetime and more importantly the finite transverse extent of the shock front will be a limiting factor when distinguishing accelerated particles from the relativistic shock heated particles.

In conclusion, it appears quite possible that diffusive shock acceleration can be reproduced in the laboratory. Even with the help of a mega-Joule laser such as NIF, an unambiguous detection of shock accelerated electrons will not be trivial, and is unlikely to be found without careful diagnostics and analysis, but should indeed be possible in the very near future. The success of such an experiment would be a first step in helping bring new insight to how Nature accelerates the most energetic particles in the Universe.

Acknowledgments

References

  [1] Amano T and Hoshino M 2007 *Astrophys. J.* **661** 190
  [2] Axford W I, Leer E and Skadron G 1977 *Proc. 15th Int. Conf. on Cosmic Rays (Plovdiv, Bulgaria, 13–26 August 1977)* vol 11 p 132
  [3] Beg F N *et al* 1997 *Phys. Plasmas* **4** 447
  [4] Bell A R 1978 *Mon. Not. R. Astron. Soc.* **182** 147
  [5] Bell A R 1978 *Mon. Not. R. Astron. Soc.* **182** 443
  [6] Bell A R 2004 *Mon. Not. R. Astron. Soc.* **353** 550
  [7] Bell A R, Schure K M and Reville B 2011 *Mon. Not. R. Astron. Soc.* **418** 1208
  [8] Bingham R, Dawson J M, Shapiro V D, Mendis D A and Kellet B J 1997 *Science* **275** 49
  [9] Blandford R and Eichler D 1987 *Phys. Rep.* **154** 1
  [10] Blandford R D and Ostriker J P 1978 *Astrophys. J. Lett.* **221** L29
  [11] Bloch F and Ross P A 1935 *Phys. Rev.* **47** 884
  [12] Courtois C *et al* 2004 *Phys. Plasmas* **11** 3386
  [13] Drake R P 2000 *Phys. Plasmas* **7** 11
  [14] Drury L O 1983 *Rep. Prog. Phys.* **46** 973

[15] Fermi E 1949 *Phys. Rev.* **75** 1169
[16] Fiuza F, Fonseca R A, Tonge J, Mori W B and Silva L O 2012 *Phys. Rev. Lett.* **108** 5004
[17] Gargaté L and Spitkovsky A 2012 *Astrophys. J.* **744** 67
[18] Gitomer S J *et al* 1986 *Phys. Fluids* **29** 2679
[19] Gregori G *et al* 2012 *Nature* **481** 480
[20] Hillas A M 1984 *Annu. Rev. Astrophys.* **22** 425
[21] Hsu S, Moser A, Dunn J, Thoma C, Adams C, Gilmore M, Lynn A, Witherspoon F D, Brockington S and van Doren D 2012 *HEDLA 2012: 9th Int. Conf. on High Energy Density Laboratory Astrophysics (Tallahassee, FL, 30 April–4 May 2012)*
[22] Huba J D 2007 *NRL Plasma Formulary* (Washington, DC: Naval Research Laboratory)
[23] Jokipii J R 1966 *Astrophys. J.* **146** 480
[24] Jokipii J R 1987 *Astrophys. J.* **313** 842
[25] Kato T N and Takabe H 2008 *Astrophys. J. Lett.* **681** L93
[26] Kirk J G and Dendy R O 2001 *J. Phys. G: Nucl. Phys.* **27** 1589
[27] Krymskii G F 1977 *Sov. Phys.—Dokl.* **22** 32
[28] Kugland N L *et al* 2012 *Nature Phys.* **8** 809
[29] Kuramitsu Y *et al* 2011 *Phys. Rev. Lett.* **106** 5002
[30] Martins S F, Fonseca R A, Silva L O and Mori W B 2009 *Astrophys. J. Lett.* **695** L189
[31] McClements K G, Dendy R O, Bingham R, Kirk J G and Drury L O'C 1997 *Mon. Not. R. Astron. Soc.* **291** 241
[32] Park H-S *et al* 2012 *High Energy Density Phys.* **8** 38
[33] Remington B A, Drake R P and Ryutov D D 2006 *Rev. Mod. Phys.* **78** 755
[34] Riquelme M A and Spitkovsky A 2011 *Astrophys. J.* **733** 63
[35] Ross J S *et al* 2012 *Phys. Plasmas* **19** 056501
[36] Ryutov D *et al* 1999 *Astrophys. J.* **518** 821
[37] Sagdeev R Z 1966 *Rev. Plasma Phys.* **4** 23
[38] Schneider H *et al* 1992 *Hyperfine Interact.* **73** 17
[39] Schwartz S J, Thomsen M F, Bame S J and Stansberry J 1988 *J. Geophys. Res.* **93** 12923
[40] Spitkovsky A 2008 *Astrophys. J. Lett.* **673** 39
[41] van Adelsberg M, Heng K, McCray R and Raymond J C 2008 *Astrophys. J.* **689** 1089
[42] Watanabe T *et al* *Phys. Rev.* **127** 2055
[43] Webb G M, Axford W I and Terasawa T 1983 *Astrophys. J.* **270** 537
[44] Woolsey N C *et al* 2001 *Phys. Plasmas* **8** 2439